HHS Public Access

Author manuscript

Eur J Immunol. Author manuscript; available in PMC 2017 September 01.

Published in final edited form as:

Eur J Immunol. 2016 September ; 46(9): 2175–2186. doi:10.1002/eji.201546201.

Type I interferon promotes alveolar epithelial type II cell survival during pulmonary *Streptococcus pneumoniae* infection and sterile lung injury in mice

Barbara B. Maier[1,2], **Anastasiya Hladik**[2], **Karin Lakovits**[2], **Ana Korosec**[1,2], **Rui Martins**[1,2], **Julia B. Kral**[3], **Ildiko Mesteri**[4], **Birgit Strobl**[5], **Mathias Müller**[5], **Ulrich Kalinke**[6,7], **Miriam Merad**[8], and **Sylvia Knapp**[1,2]

[1] CeMM – Research Center for Molecular Medicine of the Austrian Academy of Sciences, Vienna, Austria

[2] Laboratory of Infection Biology, Department of Medicine I, Medical University, Vienna, Austria

[3] Center for Physiology and Pharmacology, Institute for Physiology, Medical University of Vienna, Vienna, Austria

[4] Pathology Überlingen, Überlingen, Germany

[5] Institute of Animal Breeding and Genetics, University of Veterinary Medicine, Vienna, Austria

[6] Institute for Experimental Infection Research, TWINCORE, Center for Experimental and Clinical Infection Research, Helmholtz Center for Infection Research, Braunschweig, Germany

[7] Hannover Medical School, Hannover, Germany

[8] Department of Oncological Science, The Tisch Cancer Institute and the Immunology Institute, Mount Sinai School of Medicine, New York, New York

Abstract

Protecting the integrity of the lung epithelial barrier is essential to ensure respiration and proper oxygenation in patients suffering from various types of lung inflammation. Type I interferon (IFN-I) has been associated with pulmonary epithelial barrier function, however, the mechanisms and involved cell types remain unknown. We aimed to investigate the importance of IFN-I with respect to its epithelial barrier strengthening function to better understand immune-modulating effects in the lung with potential medical implications. Using a mouse model of pneumococcal pneumonia, we revealed that IFN-I selectively protects alveolar epithelial type II cells (AECII) from inflammation-induced cell death. Mechanistically, signaling via the IFN-I receptor on AECII is sufficient to promote AECII survival. The net effects of IFN-I are barrier protection, together with diminished tissue damage, inflammation, and bacterial loads. Importantly, we found that the protective role of IFN-I can also apply to sterile acute lung injury, in which loss of IFN-I signaling

Full correspondence: Prof. Sylvia Knapp, CeMM, Research Center for Molecular Medicine of the Austrian Academy of Sciences, and Department of Medicine I, Laboratory of Infection Biology, Medical University of Vienna Waehringer Guertel 18-20, 1090 Vienna, Austria Fax: +43-1-40400-51670, sylvia.knapp@meduniwien.ac.at.

Additional supporting information may be found in the online version of this article at the publisher's web-site

Conflict of interest: The authors declare no financial or commercial conflict of interest.

leads to a significant reduction in barrier function caused by AECII cell death. Our data suggest that IFN-I is an important mediator in lung inflammation that plays a protective role by antagonizing inflammation-associated cell obstruction, thereby strengthening the integrity of the epithelial barrier.

Keywords

Acute lung injury; Alveolar epithelial cells; Epithelial barrier; Pneumococcal pneumonia; Type I interferon

Introduction

Type I interferons (IFN-I) are strongly upregulated upon viral infections, autoimmunity, and cancer to fulfill three major functions, namely (i) inducing a cell-intrinsic antiviral state in infected cells, (ii) promoting antigen presentation and adaptive immune responses, and (iii) modulating innate inflammatory responses [1]. In many diseases the cell biology of IFN-I responses is poorly understood, since initial expression levels can be low and IFN-I secretion rapidly results in propagation of the IFN-I signal via binding to the IFN-α/β receptor (IFNAR) that is expressed on nearly all cell types [2]. In conditions of lung inflammation IFN-I are induced, thereby modulating innate immune responses by different, often ill-defined mechanisms, ranging from promotion of cell death by IFN-I [3, 4], to interference with type II IFN responses [5, 6], and shifting of macrophage phenotypes [7]. In murine pneumococcal pneumonia models, the role of IFN-I induced in the respiratory tract is controversial. A study by LeMessurier et al. [8] associated IFN-I with prevention of invasive disease and protection of pulmonary barrier function. However, Hughes et al. [9] found the expression of IFN-stimulated genes (ISGs) linked to invasiveness and blocking of IFN-I signaling could inhibit extravasation of bacteria into the pleural cavity.

In this study, we investigated the role of IFN-I in lung epithelial barrier function using pneumococcal pneumonia as a model for bacterial pneumonia and acid-induced sterile lung injury as a model for acute lung injury (ALI). *Streptococcus pneumoniae* is a Gram-positive bacterium that is the most frequent cause of community-acquired pneumonia [10]. Upon infection, a substantial inflammatory response in the lung is triggered, which rapidly escalates into systemic inflammation and life-threatening sepsis [11]. In contrast, ALI is characterized by mechanical tissue damage, caused by injury of the epithelial compartment, followed by the induction of a subsequent inflammatory response [12]. In both conditions, loss of tissue integrity leads to severe complications such as respiratory failure.

Alveolar macrophages (AMs) are known as potent IFN-I producers during respiratory viral infections, and IFN-I responsive cells are both infected cells and their bystander cells [13, 14]. In contrast, during bacterial lung infections or ALI, the IFN-I producing and responding cell types in vivo are not characterized and thus the cellular and molecular mechanism of IFN-I mediated barrier modulation is not clear. Here, we provide data generated with the help of RNA profiling and conditional IFN-I signaling deficient mice (*Ifnar1*$^{fl/fl}$) mice that allow us to identify the precise target cells of IFN-I in vivo, suggesting that AM contribute to an IFN-I response in the pathogen recognition phase of *S. pneumoniae* infection and that

IFN-I acts on alveolar epithelial type II cells (AECII). The resulting protection of AECII from cell death by IFN-I is a mechanism, which we found not only upon *S. pneumoniae* infection but also in a model of acid-induced ALI.

Results

Type I IFN prevents lung damage and bacterial dissemination during *S. pneumoniae* infection

IFN-I signaling has been linked to invasive pneumococcal pneumonia, which has been addressed by LeMessurier et al. [8], who showed that expression levels of the tight-junction proteins *Tjp1*, *Cldn5,* and *Cldn18* are reduced and the expression of *Pafr* is increased in lungs of *S. pneumoniae*-infected *Ifnar1*$^{-/-}$ mice. This strongly indicates a barrier defect in *Ifnar1*$^{-/-}$ lungs, however, the molecular and cellular mechanisms as to how IFN-I supports the epithelial barrier remain elusive. To assess the potential barrier protective role of IFN-I, we first infected WT and *Ifnar1*$^{-/-}$ mice intranasally (i.n.) with *S. pneumoniae* and analyzed bacterial numbers, cytokine levels, cell influx, and lung histology at selected time points indicative of different phases of the inflammatory response. We found lung bacterial counts increased in *Ifnar1*$^{-/-}$ mice 8 and 16 h postinfection (p.i.), corresponding to the recognition phase (8 h) and the early inflammatory phase, characterized by substantial cell recruitment and cytokine induction (16 h; Fig. 1A). Importantly, we observed systemic dissemination of bacteria as early as 8 h p.i. in *Ifnar1*$^{-/-}$ mice, reaching a significant difference at the late inflammatory phase (40 h p.i.), i.e. at a time that is characterized by inflammatory lung injury, impaired lung function, and systemic inflammation (Fig. 1A). In line with elevated bacterial counts, *Ifnar1*$^{-/-}$ mice exhibited aggravated signs of inflammation, indicated by increased levels of pulmonary and systemic CXCL1, TNF-α and IL-1β 16 and 40 h p.i. (Fig. 1B) together with a more pronounced alveolar cell influx 16 h p.i. (Fig. 1C). We excluded baseline differences in the pulmonary immune cell composition between WT and *Ifnar1*$^{-/-}$ mice by analyzing lung cell populations by flow cytometry (Supporting Information Fig. 1A–C). Upon histologic analysis of lungs 40 h p.i., we noticed more pronounced lung infiltrates in *Ifnar1*$^{-/-}$ animals (Fig. 1D), which was accompanied by a higher proportion of TUNEL-positive cells (Fig. 1E). These data suggested more severe tissue damage on a cellular level in the absence of *Ifnar1*, which was further supported by our finding of increased lung weights and elevated alveolar protein concentrations in *Ifnar1*$^{-/-}$ mice (Fig. 1F and G).

More pronounced alveolar protein levels in *Ifnar1*$^{-/-}$ mice (Fig. 1G) can be explained by the previously suggested barrierprotective role of IFN-I [8], and we could verify reduced expression levels of the tight junction components *Cldn5* and *Tjp1* in the absence of *Ifnar1* (Supporting Information Fig. 1D). Importantly, *Ifnar1*$^{-/-}$ animals showed increased lung weights and alveolar protein concentrations also after infection with heat-inactivated (HI) *S. pneumoniae*, whereas cytokine levels and cell influx were unchanged compared to control mice 40 h p.i. (Supporting Information Fig. 1E and F). These findings suggested a barrier-protective role of IFN-I independent of bacterial load and inflammation. Collectively, loss of IFN-I signaling exerted detrimental effects during pneumococcal pneumonia, illustrated by

augmented bacterial dissemination and inflammation together with more pronounced signs of epithelial barrier disruption.

IFN-I mediated protection against *S. pneumoniae* infection is via IFNAR1 signaling on AECII

Since the pulmonary epithelial barrier seems to be protected in the presence of IFN-I, we were wondering, if IFN-I acts primarily on immune cells, which in turn indirectly mediate barrier protection, or if it acts directly on epithelial cells. We, therefore, generated conditional *Ifnar1*-deficient mice to discriminate between cell types responsive to IFN-I during pneumococcal pneumonia in vivo. To this end, we crossed *Ifnar1*$^{fl/fl}$ mice with mice expressing Cre recombinase under the control of the Lysozyme M promoter, the CD11c promoter, or the SP-C promoter (active in AECII) and reduction of IFNAR1 expression on target cells was confirmed by flow cytometry (Supporting Information Fig. 2A–D). Forty hours after *S. pneumoniae* challenge, *Ifnar1*$^{fl/fl}$ *Lysm-Cre*$^{+}$ mice and *Ifnar1*$^{fl/fl}$ *Cd11c-Cre*$^{+}$ mice showed no difference in bacterial burden, inflammatory cytokine levels, or lung weight compared to *Ifnar1*$^{fl/fl}$ *Cre*$^{-}$ control mice (Fig. 2A–D). In Tamoxifen (Tx)-induced *Ifnar1*$^{fl/fl}$ *Sftpc-CreER*$^{+}$ mice we found elevated bacterial counts, higher levels of inflammatory cytokines, and higher lung weights compared to Tx-treated *Ifnar1*$^{fl/fl}$ *Cre*$^{-}$ control animals (Fig. 2E and F). Lung histological analyses revealed that inflammatory infiltrates were more pronounced in *Ifnar1*$^{fl/fl}$ *Sftpc-CreER*$^{+}$ lungs compared to *Ifnar1*$^{fl/fl}$ Cre^{-} controls after Tx treatment, whereas no difference was found in *Ifnar1*$^{fl/fl}$ *Lysm-Cre*$^{+}$ or *Ifnar1*$^{fl/fl}$ *Cd11c-Cre*$^{+}$ mice when compared to controls (Fig. 2G). Additionally, protein concentrations in BALF of *Ifnar1*$^{fl/fl}$ *Sftpc-CreER*$^{+}$ mice were elevated 16 h p.i (Fig. 2H). Hence, *Ifnar1*$^{fl/fl}$ *Sftpc-CreER*$^{+}$ mice pheno-copied conventional *Ifnar1*$^{-/-}$ mice, suggesting that IFN-I directly acts on AECII to exert its barrier protective effects.

AMs upregulate IFN-I during the onset of *S. pneumoniae* infection in vivo

Even though we could show that AECII, in contrast to immune cell populations, are the prime cells directly responding to IFN-I during pneumococcal pneumonia, we hypothesized that AMs are a source of IFN-I upon bacterial challenge in vivo, given that macrophages were shown to produce IFN-I upon *S. pneumoniae* stimulation in vitro via a mechanism dependent on bacterial uptake [15]. In vivo we detected IFN-β in *S. pneumoniae*-infected lungs as early as 8 h p.i. (Fig. 3A) which is in line with previous studies [8, 16]. At this time point AMs are the major cells phagocytosing *S. pneumoniae*, whereas neutrophils and epithelial cells are not involved in the uptake of bacteria (Supporting Information Fig. 3A and B). To test if IFN-I was induced in AM in vivo, we FACS-sorted CD45^{+}CD11c^{hi}SiglecF^{+} AMs from the BALF of *S. pneumoniae*-infected mice 3 h p.i. (Supporting Information Fig. 3C), isolated mRNA and performed a qPCR array covering IFN-I response genes. We found *Ifnb1* and *Ifna4* upregulated, together with several genes required for the augmentation of the primary IFN-I signal, e.g. *Irf9*, *Irf3*, *Stat1*, and *Ifnar1*. In contrast, genes that are involved in driving mass production of ISG, such as *Irf7* and *Stat2*, remained uninduced [2] (Fig. 3B). We verified all genes in an independent experiment using qPCR (Fig. 3C). These data show that AM internalize *S. pneumoniae* and induce IFN-I early upon infection in vivo. Upon loss of AM via i.n. treatment of mice with clodronate-filled liposomes [17], the *S. pneumoniae*-induced production of IFN-β was significantly

reduced at 8 h p.i. (Fig. 3D), despite increased cell influx and proinflammatory cytokines compared to mice treated with NaCl-filled liposomes (Supporting Information Fig. 3D and E). Sixteen hours p.i. IFN-β levels were unaffected by the loss of AM, which might be caused by repopulating AM or by other cell types (Fig. 3D).

Because it has been reported that IFN-I production in macrophages is triggered by pneumococcal DNA in vitro [16], we decided to test if the contribution of bacterial DNA also applies to the in vivo situation and infected mice with WT and DNAse-treated HI *S. pneumoniae* (ΔDNA). Doing so, pulmonary IFN-β levels and expression of the ISGs *Ifit1* and *Eif2ak2* was significantly reduced in the absence of bacterial DNA (Fig. 3E). Collectively, these findings suggest that an IFN-I response is induced in vivo upon *S. pneumoniae* infection and that bacterial DNA is a trigger of IFN-I in infected lungs.

We analyzed known parameters that have been associated with IFN-I signaling in AM to assess if *Ifnar1*$^{-/-}$ AMs are functionally altered in their response *to S. pneumoniae*. Upon stimulation with *S. pneumoniae*, *Ifnar1*$^{-/-}$ AMs showed no defects in inflammatory cytokine production and no changes in expression levels of polarization markers, indicating that *Ifnar1*$^{-/-}$ AMs are able to elicit an unaltered inflammatory response upon *S. pneumoniae* encounter (Supporting Information Fig. 3F and G). Also, the propensity of AM to undergo apoptosis was unchanged in *Ifnar1*$^{-/-}$ AM as shown by Annexin V staining as well as TUNEL assay (Supporting Information Fig. 3H and I). Taken together these data indicate that AMs from *Ifnar1*$^{-/-}$ mice are functionally unimpaired.

IFN-I signaling protects from AECII death upon *S. pneumoniae* infection

Since we discovered that IFN-I directly acts on AECII (Fig. 2E–H), we investigated the direct impact of IFN-I signaling on this cell population upon pneumococcal pneumonia. We found the expression of the AECII-specific markers *Sftpc* and *Lpcat1* reduced in *S. pneumoniae*-infected *Ifnar1*$^{-/-}$ lungs compared to infected WT lungs (Fig. 4A). Assuming that reduced marker expression might reflect loss of AECII, we performed IHC and stained for the presence of AECII in lung samples from infected mice and detected decreased numbers of proSP-C positive cells in *Ifnar1*$^{-/-}$ mice compared to WT animals. Notably, AECII also decreased upon infection in WT lungs, indicating that epithelial damage upon *S. pneumoniae* infection affects the AECII population (Fig. 4B). Importantly, *Ifnar1*$^{-/-}$ lungs infected with HI *S. pneumoniae* also showed loss of AECII marker expression (Supporting Information Fig. 4A) and reduction of proSPC positive cells shown by IHC 40 h p.i. (Fig. 4B). These data suggest that loss of AECII is caused by direct IFN-I signaling, rather than inflammatory mediators or bacterial pathogens, which were unchanged upon infection with HI *S. pneumoniae* (Supporting Information Fig. 1F). When evaluating proSP-C staining of infected lungs from conditional mice, only *Ifnar1*$^{fl/fl}$ *Sftpc-CreER*$^{+}$ mice displayed decreased numbers of AECII upon infection compared to *Ifnar1*$^{fl/lf}$ *Cre*$^{-}$ animals after Tx treatment, whereas AECII numbers were unaffected in *Ifnar1*$^{fl/fl}$ *Lysm-Cre*$^{+}$ and *Ifnar1*$^{fl/fl}$ *Cd11c-Cre*$^{+}$ mice (Supporting Information Fig. 4B). These data indicate that AECII get diminished upon *S. pneumoniae* infection and that this damage is more pronounced in the absence of IFN-I signaling on AECII.

We hypothesized that IFN-I either protects AECII from cell death or promotes their regeneration. Thus, we analyzed cell death of AECII by TUNEL assay and costained for proSP-C. *Ifnar1*$^{-/-}$ lungs exhibited a significantly higher proportion of TUNEL positive AECII, illustrating that functional IFN-I signaling indeed promoted AECII survival upon *S. pneumoniae* infection (Fig. 4C). To corroborate the direct effect of IFN-I on AECII survival we assessed the death rate of MLE cells, an AECII-derived cell line, under inflammatory conditions and in the presence or absence of IFN-β. While cell death triggered by live bacteria or pneumolysin was unaffected, most likely due to the irreversibility of pore formation, MLE cells were protected from TNF-induced cell death in the presence of IFN-β (Fig. 4D). All in all, our data suggest that IFN-I directly protects AECII from inflammation-induced cell death in vivo.

Protective effects of IFN-I signaling are also evident during sterile lung injury

To assess if the protective activity of IFN-I on AECII in vivo is confined to *S. pneumoniae* infection, we extended our studies and probed the role of *Ifnar1* during acid-induced ALI, a sterile inflammation model known to cause lung epithelial damage [12]. Eight hours after intratracheal application of hydrochloric acid, we found increased lung weights and protein concentrations in BALF of *Ifnar1*$^{-/-}$ mice (Fig. 5A). Also, the leakage of i.v.-injected Evans Blue dye into lungs was augmented in the absence of IFN-I signaling, indicating a more pronounced lung barrier defect in *Ifnar1*$^{-/-}$ mice (Fig. 5B). By studying pulmonary *Sftpc* and *Lpcat1* expression levels and proSP-C immunohistochemistry, we discovered a reduction of AECII numbers in *Ifnar1*$^{-/-}$ mice upon ALI as well as an increased proportion of dead AECII cells as indicated by higher numbers of TUNEL^{+} AECII costained for proSP-C (Fig. 5C–E). IFN-β as well as TNF were induced in lungs after ALI induction (Fig. 5F). These data suggest a broader, epithelial-protective role for IFN-I by promoting AECII survival upon inflammatory or chemical lung injury.

Discussion

The data we present here highlight a broader role for IFN-I in controlling AECII survival upon bacterial or acid-triggered lung injury, as summarized in a graphical synopsis in Figure 6. By focusing on pneumococcal pneumonia, we found support for the importance of bacterial DNA in triggering the IFN-I response in vivo and our data suggest that macrophages are a relevant early, although not the sole, source. Using conditional *Ifnar1* mice, we discovered that IFN-I signaling on AECII, but not on major immune cell populations, was sufficient to strengthen the pulmonary epithelial barrier. The net effect of IFN-I's activity was barrier protection together with the reduction of local and systemic inflammation and bacterial load. Further, by revealing that IFN-I protected AECII not only from *S. pneumoniae* but also ALI-induced cell death in vivo, we propose a wider and beneficial role for IFN-I in safeguarding the lung epithelial barrier in settings of acute lung damage.

Our findings, in which IFN-I restrains inflammation-induced epithelial damage, extend and corroborate earlier reports that described epithelial barrier-protective properties elicited by IFN-I [8]. LeMessurier et al. [8] showed that expression levels of tight junction proteins

were reduced in the lungs of *S. pneumoniae*-infected *Ifnar1*$^{-/-}$ mice, which they found associated with more pronounced bacterial spread. Treatment with recombinant IFN-β resulted in increased expression of tight junction proteins and local containment of bacteria. We were able to reproduce this phenotype and further provide evidence that loss of IFN-I signaling specifically on AECII not only led to a decrease in epithelial tight junction proteins, but also a reduction of the AECII compartment itself caused by increased cell death of this population. We consider these findings an important extension of current knowledge on the IFN-I dependent maintenance of the pulmonary barrier function during inflammation. Interestingly, in a study by Hughes et al. [9] treatment with a blocking antibody directed against IFNAR1 inhibited pneumococcal colonization of the pleural cavity 6 h p.i., an effect that was lost 24 h p.i. Bacterial counts in the lung and blood were unaffected by systemic IFNAR1 blocking [9]. This could indicate on the one hand that an IFN-I dependent mechanism for bacterial spread specific for the pleural cavity exists, which might be independent from our observations that IFN-I signaling supports the AECII compartment. On the other hand the capsular serotype of *S. pneumoniae* used in this study differs from the serotype of the strain we were using, which could explain different invasive capacities, since the pneumococcal capsule is known to be an important factor defining efficiency of epithelial adhesion and transmigration [18].

IFN-Is are well known to contribute to hematopoietic stem cell renewal [19] and it is important to reconsider that also the AECII compartment exhibits stem cell characteristics important for the regeneration of alveolar epithelial type I cells [20, 21]. It is therefore of great significance for the host to protect this cell population in order to ensure the integrity and renewal capacity of alveoli that are damaged during inflammatory responses. This aspect is of particular relevance in patients suffering from ALI-associated respiratory failure, as is our observation that IFN-I executes barrier-strengthening effects in a model of ALI. It is tempting to speculate that potential treatments that preserve AEC-II viability will not only protect the epithelial barrier, but also subsequently support the regeneration of the alveolar lining.

Another clinically important condition, where patients might benefit from treatments that support the epithelial barrier, is postinfluenza bacterial pneumonia. In this setting IFN-I has been shown to play a major, albeit detrimental role for the host [22, 23]. Interestingly, in contrast to our study IFN-I has been demonstrated to promote apoptosis of the alveolar epithelium in response to Influenza virus [24–26]. These studies in conjunction with the data we report here support the attractive possibility that IFN-I acts as a context-specific regulator of epithelial cell viability in the lungs. As such, IFN-I differentiates between situations in which the host benefits from tissue protection to keep alveolar damage under control, i.e. a bacterial infection or sterile inflammation, and conditions in which epithelial cells are infected by respiratory viruses and need to be eliminated [27–29]. Thus, we speculate that IFN-I mediated enhancement of epithelial cell death upon viral infection likely contributes to the worsened pneumonia outcome observed in superinfected mice. Most bacterial superinfection data are based on settings in which mice receive *S. pneumoniae* at the peak of influenza-induced IFN-I secretion [22]. In this context IFN-I promotes epithelial cell apoptosis, leading to enhanced tissue damage and barrier disruption that most likely facilitates bacterial dissemination and aggravates lung damage upon bacterial coinfection.

Cell homeostasis in the intestinal epithelium was shown to be regulated by IFN-I. *Ifnar1*$^{fl/fl}$ *Villin-Cre* mice, depleted specifically for *Ifnar1* in the intestinal epithelium, exhibit a decreased number of Paneth and goblet cells and an increased proliferation of intestinal epithelial cells at baseline [30]. Those changes are dependent on the intestinal microflora and can be reversed when *Ifnar1*$^{fl/fl}$ *Villin-Cre* mice are cohoused with WT animals. Antibiotic-treated or germ-free mice show substantial degrees of epithelial degeneration, lower pulmonary *Ifnb* expression, and impaired adaptive immune responses upon influenza infection, which can be partially restored by administering pI:C, a potent trigger of IFN-I [31]. The exact causative relationship between IFN-I, pulmonary epithelium, and lung microflora still remains to be investigated. Taking into account that IFN-I plays an important role in the regulation of the pulmonary epithelium ([24], and our data), impacts on microbiota [30] and the host's microbiota being crucial for mounting IFN-I responses [31], we hypothesize that IFN-I and the microbiota could represent two important interdependent factors not only involved in the priming of immune cell populations in the lung, but also in controlling the functionality of the alveolar epithelium.

Materials and methods

Ethics statement

All mouse experiments were performed after approval by the Institutional Review Board of the Medical University of Vienna and the Austrian Ministry of Sciences in accordance with Austrian law (BMWF-66.009/0284-WF/V/3b/2014). All experiments were performed under anesthesia with a mixture of ketamine (100 mg/kg) and xylazine (20 mg/kg) and all efforts were made to reduce, refine, and replace animal experiments.

Mice

Eight-week-old female mice on the C57BL/6 background were used for all experiments. Ifnar$^{fl/fl}$ mice [32] were crossed with Lysm-Cre$^{+/-}$ mice [33], Cd11c-Cre$^{+/-}$ mice [34], or Sftpc-CreER$^{+/-}$ mice [35] (kindly provided by Prof. Brigid Hogan). Littermate Cre^{+} and Cre^{-} mice were used for experiments. *Ifnar1*$^{-/-}$ mice [36] were compared to WT control mice.

Bacterial strains and infection models

Mice were infected with the indicated doses of *S. pneumoniae* as previously described [37, 38]. *Streptococcus pneumoniae* strain ATCC 6303 was used for all experiments, unless indicated otherwise. GFP^{+} *S. pneumoniae* were on the D39 background and respective WT D39 control strains were used. Bacteria were incubated at 65°C for 30 min for HI. DNAse treatment of HI bacteria was performed with DNAse I (Sigma) for 1 h at 37°C followed by DNAse inactivation by incubation at 75°C for 10 min. Eight, 16, or 40 h p.i. mice were sacrificed with a mixture of ketamine and xylazine and organ samples were collected. BALF was taken in some experiments by flushing the lung with 1 mL of sterile NaCl as described earlier [39]. Giemsa-stained cytospin preparations of BALF were used for differential cell counts. Total protein in BALF was determined by Pierce BCA Protein Assay Kit (Thermo Scientific). Lungs were homogenized using Precellys 24TM (Peqlab) and bacterial counts were quantified by plating tenfold serial dilutions of lungs and blood on blood agar plates.

Protein was extracted from remaining lung homogenates as described earlier [37]. ELISA kits for mouse TNF-α, IL-1β, and CXCL1 were purchased from R&D Systems, the ELISA kit for mouse IFN-β was purchased from PBL IFN source.

Ten days prior to infection, Tx-inducible Cre was activated by i.p. injecting 5 mg Tx (Sigma) dissolved in corn oil on four consecutive days. For AM depletion, 50 μL of either Clodronate-filled liposomes or NaCl-filled liposomes (ClodronateLiposomes.com) were applied to mice i.n. 2 days prior to infection.

Histology, immunohistochemistry, and immunofluorescence

For histologic examination lungs were fixed in 7.5% formaldehyde and embedded in paraffin. Hematoxylin and eosin-stained sections were analyzed by a pathologist. Lung damage was scored as described earlier [40]. For proSP-C immunostaining, endogenous peroxidase activity was quenched and antigen was retrieved with Antigen Unmasking Solution (Vector, H-3300). Blocking was done in normal goat serum and the slides were stained with antiproSP-C (Abcam, ab40879). A secondary goat-anti-rabbit antibody (Vector Lab, BA-1000) was applied and the signal was amplified with Vectastain ABC kit (Vector, PK-6100) and Peroxidase Substrate Kit (Vector, SK-4100) was applied. Cell structures were stained with hematoxylin and pictures were taken on an Olympus FSX100 Microscope. For analysis, ten pictures per lung were taken and manually screened for proSP-C^+ cells per field. For TUNEL staining, slides were stained with TUNEL reaction mix (Roche, In situ cell death detection kit, AP, 11684809910). Nuclei were stained with DAPI and slides were kept in Prolong Antifade Reagent (Life Technologies P36930). Automatic image analysis with CellProfiler software was performed to quantify TUNEL stain [41] (http://www.cellprofiler.org). CellProfiler was programed to: (i) split images into channels; (ii) load the channels into the pipeline and identify primary objects (DAPI) using the Otsu adaptive method with two-class thresholding (threshold range 0.14–1), minimized weighted variance, and intensity method to distinguish clumped objects; and (iii) retrieve the respective DAPI and TUNEL integrated intensities of each identified nucleus. The integrated DAPI and TUNEL intensities were then normalized to the average DAPI integrated intensity. For TUNEL and proSP-C costaining, slides were stained with TUNEL reaction mix as described above, blocked with normal goat serum and stained for proSP-C as described above. Pictures were taken on a Zeiss Axioimager microscope. For analysis, ten pictures per lung were taken and manually screened for $TUNEL^+$ proSP-C^+ cells per field.

qRT-PCR and RNA profiling

RNA was isolated from cells using TRIzol Reagent (Invitrogen) and from tissues using a commercial kit (Macherey–Nagel). Quantitative RT-PCR was performed using iTaq SYBR Green Supermix (Bio-Rad). Data are presented as fold change over the appropriate control group, i.e. mock-infected mice or vehicle-treated cells, respectively. A list of primers is included in Supporting Information Table 1. For RNA profiling, the RT^2 Profiler Array "Type I Interferon Response" (Qiagen Cat. No. 330231 PAMM-016ZA) was used. Data are presented as fold change over AM sorted from mock-infected mice.

Flow cytometry

For Annexin V staining cells retrieved from BALF were stained with Annexin V-FITC Apoptosis Detection Kit (eBioscience) and 7-AAD Viability Dye (eBioscience).To prepare whole lung cell suspensions, lungs were perfused with PBS and digested in RPMI containing 5% FCS, 150 U/mL collagenase type I (Gibco, Cat. No. 17100), and 50 U/mL DNAse I (Sigma) for 40 min at 37°C. Single-cell suspensions were obtained by flushing the samples through a 70 μm filter. Viability of cells was assessed using either DAPI or Fixable Viability Dye eFluor 780 (eBioscience). A list of antibodies is included in the Supporting Information Table 2. Flow cytometry and sorting was performed using a BD LSRFortessa, and data were analyzed using the FlowJo software version 10.

Cell culture and stimulations

AMs were isolated from BALF [37] and cultured in RPMI containing 10% fetal calf serum (FCS) and 1% penicillin and streptomycin. All stimulations were carried out in medium containing 3% FCS. HI *S. pneumoniae* were used for stimulations at a concentration of 10^7 CFU/mL. Supernatants of stimulated cells were used for cytokine quantification and cells were taken up in 100 μL Trizol for RNA extraction. Immortalized mouse lung epithelial cells 12 (MLE-12) cells were cultured in RPMI containing 2% FCS, 1% penicillin and streptomycin, 0.5% insulin-transferrin-sodiumselenite, 5 mg/L transferrin, 10 nM hydrocortisone, and 10 nM β-estradiol. All stimulations were carried out in this medium without FCS. Cells were pretreated with recombinant IFN-β (BioLegend) at a concentration of 1 ng/mL for 30 min. Purified pneumolysin (MyBioSource) was used at a concentration of 10 ng/mL. Recombinant TNF-α (BioLegend) was used at a concentration of 5 μg/mL. Viable *S. pneumoniae* was used for stimulations at a concentration of 5×10^5 CFU/mL and HI *S. pneumoniae* was used at 10^7 CFU/mL. Cells were lysed in CellTiter-Glo reagent (Promega, CellTiter-Glo Luminescent Cell Viability Assay) and viability was assessed with a Glomax 96 Microplate Luminometer (Promega).

Sterile lung injury

Sixty microliters of 0.1 N HCL (Sigma) was instilled intratracheally into anesthetized mice with the help of an otoscope. After 8 h, mice were sacrificed with a mixture of ketamine and xylazine. BALF was collected and lungs were removed and homogenized as described above. In some experiments 750 μg Evans Blue (Sigma) was injected i.v. 7.5 h after acid aspiration. Evans Blue extravasation was directly measured from BALF at OD_{620}. Lung tissue was placed into 2 mL formamide (Sigma) for 2 days at RT to extract Evans Blue dye, which was quantified using a photospectrometer at OD_{620}. A standard curve for Evans Blue dissolved in formamide at known concentrations was used to determine total amount of extracted dye from tissues. Lungs and BALF from mice not injected with Evans Blue were used to correct for hemoglobin present in the tissue. Data were normalized to mock-treated, Evans Blue-injected mice.

Statistics

Comparisons between groups were performed using unpaired, two-sided *t*-test or one-way ANOVA followed by Tukey's multiple comparisons analysis, where appropriate. Sample

sizes for in vivo experiments were calculated based on previous experience. Data are presented as mean ± SD.

Supplementary Material

Refer to Web version on PubMed Central for supplementary material.

Acknowledgments

We thank Brigid L.M. Hogan and Dagmar Stoiber for generously providing us with mouse strains. This work was supported by the Austrian Science Fund FWF (W1205 to S.K. and SFB F28 to M.Mü. and B.S.), and Infect-ERA via the Austrian Science Fund FWF (I 1620-B22 to S.K.).

Abbreviations

AECII	alveolar epithelial type II cells
ALI	acute lung injury
AM	alveolar macrophage
HI	heat inactivation
ISG	IFN-stimulated genes
p.i.	postinfection
Tx	tamoxifen

References

1. Trinchieri G. Type I interferon: friend or foe? J. Exp. Med. 2010; 207:2053–2063. [PubMed: 20837696]
2. Ivashkiv LB, Donlin LT. Regulation of type I interferon responses. Nat. Rev. Immunol. 2014; 14:36–49. [PubMed: 24362405]
3. Carrero JA, Calderon B, Unanue ER. Lymphocytes are detrimental during the early innate immune response against Listeria monocytogenes. J. Exp. Med. 2006; 203:933–940. [PubMed: 16549598]
4. Qiu H, Fan Y, Joyee AG, Wang S, Han X, Bai H, Jiao L, et al. Type I IFNs enhance susceptibility to *Chlamydia muridarum* lung infection by enhancing apoptosis of local macrophages. J. Immunol. 2008; 181:2092–2102. [PubMed: 18641348]
5. Rothfuchs AG, Trumstedt C, Mattei F, Schiavoni G, Hidmark A, Wigzell H, Rottenberg ME. STAT1 regulates IFN-alpha beta- and IFN-gamma-dependent control of infection with *Chlamydia pneumoniae* by nonhemopoietic cells. J. Immunol. 2006; 176:6982–6990. [PubMed: 16709859]
6. Teles RM, Graeber TG, Krutzik SR, Montoya D, Schenk M, Lee DJ, Komisopoulou E, et al. Type I interferon suppresses type II interferon-triggered human anti-mycobacterial responses. Science. 2013; 339:1448–1453. [PubMed: 23449998]
7. Plumlee CR, Lee C, Beg AA, Decker T, Shuman HA, Schindler C. Interferons direct an effective innate response to *Legionella pneumophila* infection. J. Biol. Chem. 2009; 284:30058–30066. [PubMed: 19720834]
8. LeMessurier KS, Hacker H, Chi L, Tuomanen E, Redecke V. Type I interferon protects against pneumococcal invasive disease by inhibiting bacterial transmigration across the lung. PLoS Pathog. 2013; 9:e1003727. [PubMed: 24244159]

9. Hughes CE, Harvey RM, Plumptre CD, Paton JC. Development of primary invasive pneumococcal disease caused by serotype 1 pneumococci is driven by early increased type I interferon response in the lung. Infect. Immun. 2014; 82:3919–3926. [PubMed: 25001606]
10. Musher DM, Thorner AR. Community-acquired pneumonia. N. Engl. J. Med. 2014; 371:1619–1628. [PubMed: 25337751]
11. Koppe U, Suttorp N, Opitz B. Recognition of *Streptococcus pneumoniae* by the innate immune system. Cell. Microbiol. 2012; 14:460–466. [PubMed: 22212419]
12. Matute-Bello G, Frevert CW, Martin TR. Animal models of acute lung injury. Am. J. Physiol. Lung Cell. Mol. Physiol. 2008; 295:L379–L399. [PubMed: 18621912]
13. Divangahi M, King IL, Pernet E. Alveolar macrophages and type I IFN in airway homeostasis and immunity. Trends Immunol. 2015; 36:307–314. [PubMed: 25843635]
14. Kallfass C, Lienenklaus S, Weiss S, Staeheli P. Visualizing the beta interferon response in mice during infection with influenza A viruses expressing or lacking nonstructural protein 1. J. Virol. 2013; 87:6925–6930. [PubMed: 23576514]
15. Koppe U, Hogner K, Doehn JM, Muller HC, Witzenrath M, Gutbier B, Bauer S, et al. *Streptococcus pneumoniae* stimulates a STING- and IFN regulatory factor 3-dependent type I IFN production in macrophages, which regulates RANTES production in macrophages, cocultured alveolar epithelial cells, and mouse lungs. J. Immunol. 2012; 188:811–817. [PubMed: 22156592]
16. Parker D, Martin FJ, Soong G, Harfenist BS, Aguilar JL, Ratner AJ, Fitzgerald KA, et al. *Streptococcus pneumoniae* DNA initiates type I interferon signaling in the respiratory tract. MBio. 2011; 2:e00016–11. [PubMed: 21586648]
17. Knapp S, Leemans JC, Florquin S, Branger J, Maris NA, Pater J, van Rooijen N, et al. Alveolar macrophages have a protective antiinflammatory role during murine pneumococcal pneumonia. Am. J. Respir. Crit. Care Med. 2003; 167:171–179. [PubMed: 12406830]
18. Kadioglu A, Weiser JN, Paton JC, Andrew PW. The role of *Streptococcus pneumoniae* virulence factors in host respiratory colonization and disease. Nat. Rev. Microbiol. 2008; 6:288–301. [PubMed: 18340341]
19. Essers MA, Offner S, Blanco-Bose WE, Waibler Z, Kalinke U, Duchosal MA, Trumpp A. IFNalpha activates dormant haematopoietic stem cells in vivo. Nature. 2009; 458:904–908. [PubMed: 19212321]
20. Barkauskas CE, Cronce MJ, Rackley CR, Bowie EJ, Keene DR, Stripp BR, Randell SH, et al. Type 2 alveolar cells are stem cells in adult lung. J. Clin. Invest. 2013; 123:3025–3036. [PubMed: 23921127]
21. Desai TJ, Brownfield DG, Krasnow MA. Alveolar progenitor and stem cells in lung development, renewal and cancer. Nature. 2014; 507:190–194. [PubMed: 24499815]
22. Shahangian A, Chow EK, Tian X, Kang JR, Ghaffari A, Liu SY, Belperio JA, et al. Type I IFNs mediate development of postinfluenza bacterial pneumonia in mice. J. Clin. Invest. 2009; 119:1910–1920. [PubMed: 19487810]
23. Davidson S, Maini MK, Wack A. Disease-promoting effects of type I interferons in viral, bacterial, and coinfections. J. Interferon Cytokine Res. 2015; 35:252–264. [PubMed: 25714109]
24. Hogner K, Wolff T, Pleschka S, Plog S, Gruber AD, Kalinke U, Walmrath HD, et al. Macrophage-expressed IFN-beta contributes to apoptotic alveolar epithelial cell injury in severe influenza virus pneumonia. PLoS Pathog. 2013; 9:e1003188. [PubMed: 23468627]
25. Herold S, Steinmueller M, von Wulffen W, Cakarova L, Pinto R, Pleschka S, Mack M, et al. Lung epithelial apoptosis in influenza virus pneumonia: the role of macrophage-expressed TNF-related apoptosis-inducing ligand. J. Exp. Med. 2008; 205:3065–3077. [PubMed: 19064696]
26. Ishikawa E, Nakazawa M, Yoshinari M, Minami M. Role of tumor necrosis factor-related apoptosis-inducing ligand in immune response to influenza virus infection in mice. J. Virol. 2005; 79:7658–7663. [PubMed: 15919918]
27. Fujimoto I, Pan J, Takizawa T, Nakanishi Y. Virus clearance through apoptosis-dependent phagocytosis of influenza A virus-infected cells by macrophages. J. Virol. 2000; 74:3399–3403. [PubMed: 10708457]

28. Tyrrell C, McKechnie SR, Beers MF, Mitchell TJ, McElroy MC. Differential alveolar epithelial injury and protein expression in pneumococcal pneumonia. Exp. Lung Res. 2012; 38:266–276. [PubMed: 22563685]
29. Canvin JR, Marvin AP, Sivakumaran M, Paton JC, Boulnois GJ, Andrew PW, Mitchell TJ. The role of pneumolysin and autolysin in the pathology of pneumonia and septicemia in mice infected with a type 2 pneumococcus. J. Infect. Dis. 1995; 172:119–123. [PubMed: 7797901]
30. Tschurtschenthaler M, Wang J, Fricke C, Fritz TM, Niederreiter L, Adolph TE, Sarcevic E, et al. Type I interferon signalling in the intestinal epithelium affects Paneth cells, microbial ecology and epithelial regeneration. Gut. 2014; 63:1921–1931. [PubMed: 24555997]
31. Abt MC, Osborne LC, Monticelli LA, Doering TA, Alenghat T, Sonnenberg GF, Paley MA, et al. Commensal bacteria calibrate the activation threshold of innate antiviral immunity. Immunity. 2012; 37:158–170. [PubMed: 22705104]
32. Kamphuis E, Junt T, Waibler Z, Forster R, Kalinke U. Type I interferons directly regulate lymphocyte recirculation and cause transient blood lymphopenia. Blood. 2006; 108:3253–3261. [PubMed: 16868248]
33. Clausen BE, Burkhardt C, Reith W, Renkawitz R, Forster I. Conditional gene targeting in macrophages and granulocytes using LysMcre mice. Transgenic Res. 1999; 8:265–277. [PubMed: 10621974]
34. Caton ML, Smith-Raska MR, Reizis B. Notch-RBP-J signaling controls the homeostasis of CD8- dendritic cells in the spleen. J. Exp. Med. 2007; 204:1653–1664. [PubMed: 17591855]
35. Rock JR, Barkauskas CE, Cronce MJ, Xue Y, Harris JR, Liang J, Noble PW, et al. Multiple stromal populations contribute to pulmonary fibrosis without evidence for epithelial to mesenchymal transition. Proc. Natl. Acad. Sci. USA. 2011; 108:E1475–E1483. [PubMed: 22123957]
36. Muller U, Steinhoff U, Reis LF, Hemmi S, Pavlovic J, Zinkernagel RM, Aguet M. Functional role of type I and type II interferons in antiviral defense. Science. 1994; 264:1918–1921. [PubMed: 8009221]
37. Warszawska JM, Gawish R, Sharif O, Sigel S, Doninger B, Lakovits K, Mesteri I, et al. Lipocalin 2 deactivates macrophages and worsens pneumococcal pneumonia outcomes. J. Clin. Invest. 2013; 123:3363–3372. [PubMed: 23863624]
38. Sharif O, Matt U, Saluzzo S, Lakovits K, Haslinger I, Furtner T, Doninger B, et al. The scavenger receptor CD36 downmodulates the early inflammatory response while enhancing bacterial phagocytosis during pneumococcal pneumonia. J. Immunol. 2013; 190:5640–5648. [PubMed: 23610144]
39. Knapp S, Wieland CW, van 't Veer C, Takeuchi O, Akira S, Florquin S, van der Poll T. Toll-like receptor 2 plays a role in the early inflammatory response to murine pneumococcal pneumonia but does not contribute to antibacterial defense. J. Immunol. 2004; 172:3132–3138. [PubMed: 14978119]
40. Lagler H, Sharif O, Haslinger I, Matt U, Stich K, Furtner T, Doninger B, et al. TREM-1 activation alters the dynamics of pulmonary IRAK-M expression in vivo and improves host defense during pneumococcal pneumonia. J. Immunol. 2009; 183:2027–2036. [PubMed: 19596984]
41. Carpenter AE, Jones TR, Lamprecht MR, Clarke C, Kang IH, Friman O, Guertin DA, et al. CellProfiler: image analysis software for identifying and quantifying cell phenotypes. Genome Biol. 2006; 7:R100. [PubMed: 17076895]

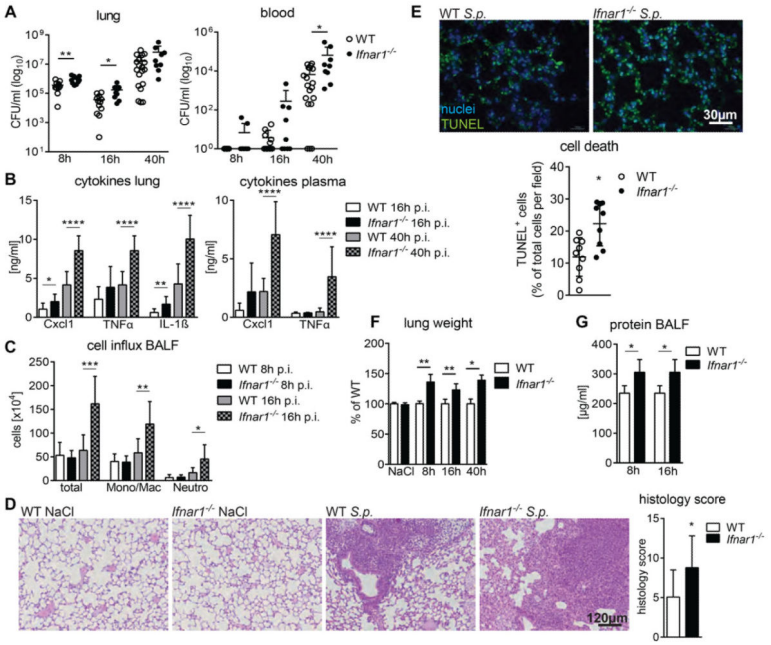

Figure 1.

Loss of IFN-I signaling aggravates the pathology of pneumococcal pneumonia. WT and *Ifnar1*$^{-/-}$ mice were infected i.n. with 10^5 CFU *S. pneumoniae* (ATCC 6303) and sacrificed at 8, 16, or 40 h p.i. (A) Bacterial load was assessed in the lungs and blood. (B) Cytokines of homogenized organs (left panel) or plasma (right panel) were quantified by ELISA. (C) Differential cell counts of BALF cells were done on cytospin preparations. (D) H&E staining of lung tissue and histology score of the staining on the right. (E) TUNEL staining of WT (left panel) and *Ifnar1*$^{-/-}$ lungs (right panel) 40 h p.i. and quantification of TUNEL$^+$ cells per field (lower panel). (F) Lung weight in WT and *Ifnar1*$^{-/-}$ mice at 8, 16, and 40 h p.i. (G) Protein levels in the BALF at 8 and 16 h p.i. Data from one experiment are shown as mean + SD and are representative for two independent experiments, with eight mice per group per experiment. Two-sided *t*-test was performed to test for statistical significance. *$p \leq 0.05$, **$p \leq 0.01$, ***$p \leq 0.001$, ****$p \leq 0.0001$. Images in (D) and (E) are representative of two independent experiments, with eight mice per group per experiment; (10x magnification (D) and 40x (E)).

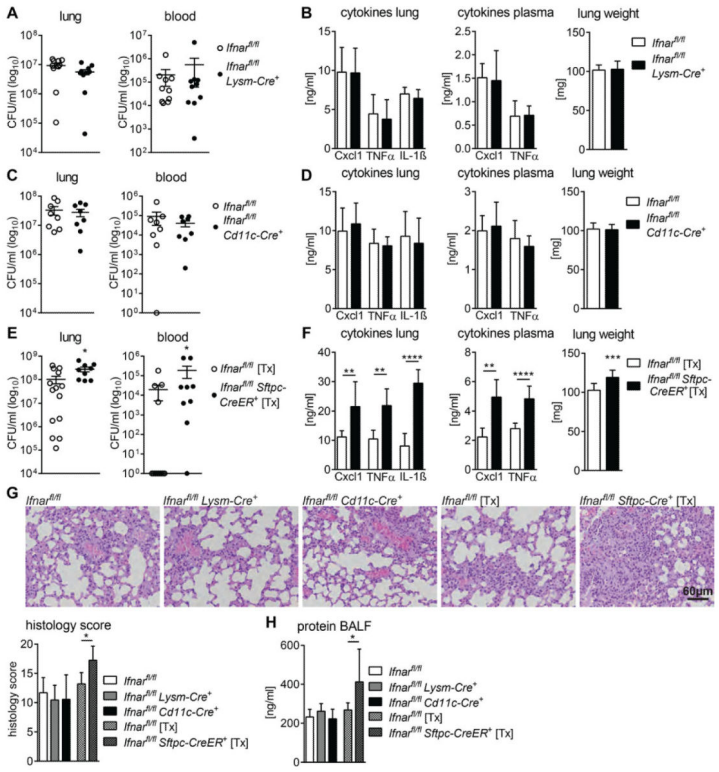

Figure 2.

IFN-I acting on AECII prevents bacterial dissemination and damage during pneumococcal pneumonia. *Ifnar*$^{fl/fl}$, *Ifnar*$^{fl/fl}$ *Lysm-Cre*$^{+}$, *Ifnar*$^{fl/fl}$ *Cd11c-Cre*$^{+}$, or *Ifnar*$^{fl/fl}$ *Sftpc-CreER*$^{+}$ mice were infected i.n. with 10^5 CFU *S. pneumoniae* (ATCC 6303). (A–H) At 40 h p.i., the (A, C, and E) bacterial loads in lungs and blood and (B, D, and F) cytokine levels in lung, plasma, and lung weight were assessed for *Ifnar*$^{fl/fl}$, in comparison against (A and B) *Ifnar*$^{fl/fl}$ *Lysm-Cre*$^{+}$, (C and D) *Ifnar*$^{fl/fl}$ *Cd11c-Cre*$^{+}$, or (E and F) *Ifnar*$^{fl/fl}$ *Sftpc-CreER*$^{+}$ mice. (F and G) *Ifnar*$^{fl/fl}$ and *Ifnar*$^{fl/fl}$ *Sftpc-CreER*$^{+}$ mice were injected with 5 mg Tx on four consecutive days and infected 10 days after the last Tx injection. (G) Images (upper panels) represent H&E staining of lung tissue sections at 40 h p.i. (20x magnification). Histology score (lower panel). Images are representative of two independent experiments, with six mice per group per experiment. (H) Protein concentrations were quantified in the BALF at 16 h p.i. Data from one experiment are shown as mean + SD and are representative for two independent experiments, with eight mice per group per experiment. Two-sided *t*-test was performed to test for statistical significance. *$p \leq 0.05$, **$p \leq 0.01$, ***$p \leq 0.001$, ****$p \leq 0.0001$.

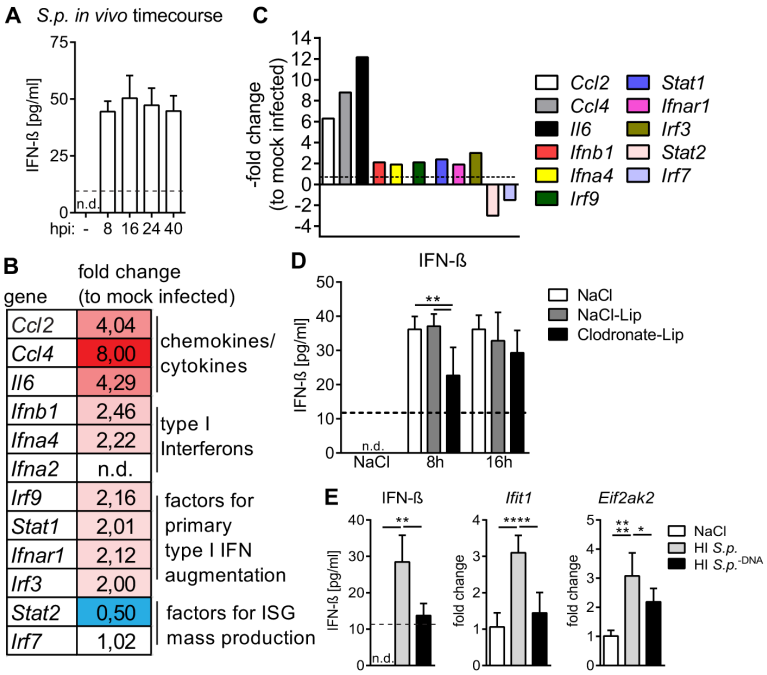

Figure 3.

AMs upregulate IFN-I and factors necessary for IFN-I expression upon *S. pneumoniae* infection. (A and B) WT mice were infected i.n. with 10^5 CFU *S. pneumoniae* (ATCC 6303) (A) IFN-β was quantified in lung homogenates by ELISA at the indicated time points. (B) BALF was taken 3 h p.i., AMs were sorted by flow cytometry, and qRT-PCR array was performed on the extracted RNA (AMs were pooled from three mice per group) (C) As in Figure 3B, AM of infected WT mice were sorted by flow cytometry and qRT-PCR for the indicated genes was performed on the extracted RNA. (D) Mice were treated i.n. with 50 μL Clodronate-filled liposomes, NaCl-filled liposomes, or NaCl 2 days prior to infection with 10^5 CFU *S. pneumoniae* (ATCC 6303). Lungs were harvested at indicated timepoints and IFN-β levels were assessed by ELISA. (E) Mice were infected with 10^7 CFU HI *S. pneumoniae* or DNAse-treated HI *S. pneumoniae* (both D39). Forty hours p.i. lung homogenates of WT mice were analyzed for IFN-β by ELISA (left panel), and for *Ifit1* (middle panel) and *Eif2ak2* (right panel) by qRT-PCR. Dashed lines (A, D, and E) indicate the detection limit. Data are shown as mean + SD. The qRT-PCR array in (B) was performed once with three mice per experiment and all depicted genes were validated by qRT-PCR in an independent experiment (C) with three mice per experiment. In (A, D, and E), data from one experiment are shown and are representative for two experiments with eight mice per group per experiment. In (D and E) one-way ANOVA followed by Tukey's multiple comparisons analysis was performed to test for statistical significance. $*p \leq 0.05$, $**p \leq 0.01$, $***p \leq 0.001$, $****p \leq 0.0001$.

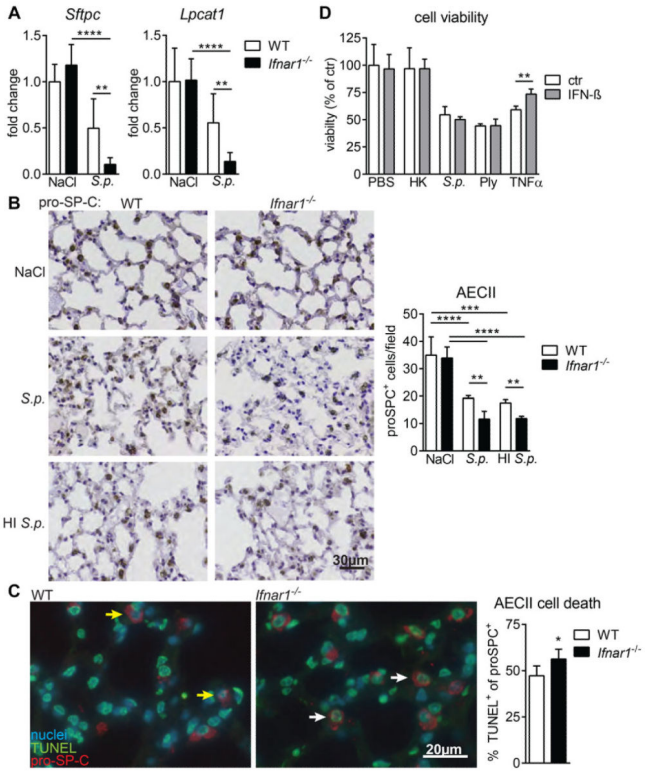

Figure 4.

IFN-I signaling maintains AECII numbers and prevents AECII cell death upon pneumococcal pneumonia. WT and *Ifnar1*$^{-/-}$ mice were infected i.n. with 10^5 CFU *S. pneumoniae* (ATCC 6303) or with 10^7 CFU HI *S. pneumoniae* (ATCC 6303; $n \geq 8$ for each group). (A) Forty hours p.i. *Sftpc* (left panel) and *Lpcat1* (right panel) levels were quantified by qRT-PCR from lung homogenates, (B) paraffin-embedded lung tissue from WT mice (left panel) and *Ifnar1*$^{-/-}$ mice (right panel) was stained for proSP-C, and (C) costained for proSP-C and TUNEL; yellow arrows indicate proSP-C$^+$ TUNEL$^-$ cells and white arrows indicate pro-SP-C$^+$ TUNEL$^+$ cells. Quantifications of the histology are shown on the right in (B and C), respectively. (D) Serum-starved MLE cells were pretreated with 1 ng/mL IFN-β for 30 min and subsequently stimulated with 10 ng/mL pneumolysin (Ply), 5×10^5 CFU/mL *S. pneumoniae* ATCC 6303 (S.p.), 10^7 CFU/mL HI *S. pneumoniae* ATCC 6303 (HI), or 5 µg/mL TNF-α. After 4 h cell survival was measured. Images and quantification in (B and C) are representative of two independent experiments, with eight mice per group per experiment (40x), In vitro stimulations were performed in quadruplicates. Data from one experiment are shown as mean + SD and are representative for two experiments with eight mice per group per experiment. Two-sided *t*-test was performed to test for statistical significance. *$p \leq 0.05$, **$p \leq 0.01$, ***$p \leq 0.001$, ****p s 0.0001.

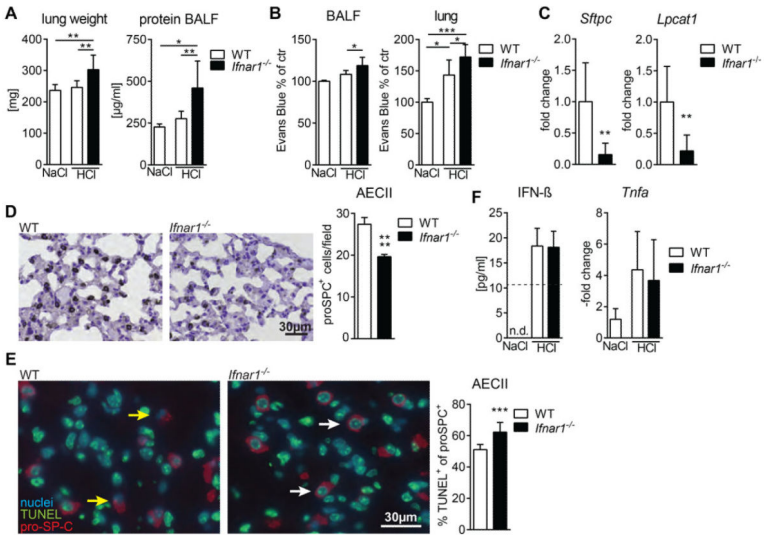

Figure 5.

Absence of IFN-I signaling is linked to reduced AECII numbers upon acid induced lung injury. HCl was instilled i.t. into WT and *Ifnar1*$^{-/-}$ mice and all mice were sacrificed 8 h later. (A) Lung weight (left panel) and protein concentrations (right panel) in BALF were assessed. (B) Some mice received Evans Blue i.v. 60 min before BALF and lungs were collected. Evans Blue was quantified in BALF (left panel) and formamide-pretreated lungs (right panel). (C) *Sftpc* (left panel) and *Lpcat1* (right panel) were quantified by qRT-PCR from lung tissues. (D) Paraffin-embedded lung tissue was stained for *proSP-C* and (E) costained for proSP-C and TUNEL; yellow arrows indicate proSP-C^{+} TUNEL^{-} cells and white arrows indicate pro-SP-C^{+} TUNEL^{+} cells. Quantifications of the histology are shown on the right. Images and quantification in (C and E) are representative of two independent experiments, with eight mice per group per experiment (40x). (F) Lung homogenates were analyzed for IFN-β by ELISA and for *Tnfa* by qRT-PCR. Dashed lines indicate the detection limit. In vitro stimulations were performed in quadruplicates. Data from one experiment are shown as mean + SD and are representative for two experiments with eight mice per group per experiment. Two-sided *t*-test or one-way ANOVA followed by Tukey's multiple comparisons analysis was performed to test for statistical significance. *$p \leq 0.05$, **$p \leq 0.01$, ***$p \leq 0.001$, ****$p \leq 0.0001$.

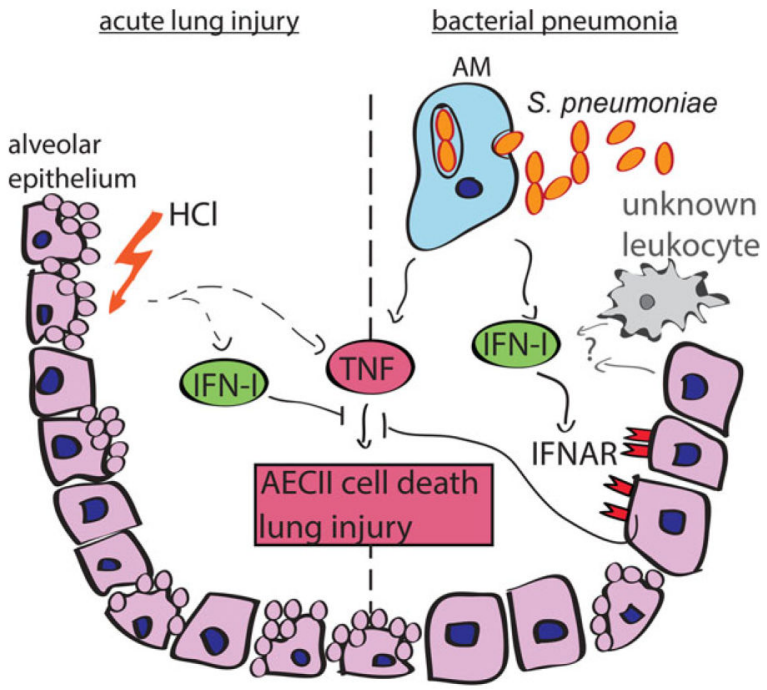

Figure 6.

Proposed model of IFN-I mediated protective effects on AECII. Upon infection, AMs encounter and ingest *S. pneumoniae* to then induce an inflammatory response that involves secretion of IFN-I. In a similar manner, sterile ALI is associated with tissue damage and resulting inflammation. Respiratory epithelial cells are damaged in the course of pulmonary inflammation, which is diminished in the presence of IFN-I, which directly protects AECII from death.